JCTC Journal of Chemical Theory and Computation

Fully Relativistic, Comparative Investigation of Gold and Platinum Alkyne Complexes of Relevance for the Catalysis of Nucleophilic Additions to Alkynes

Markus Pernpointner*,† and A. Stephen K. Hashmi‡

Theoretische Chemie, Universität Heidelberg, Im Neuenheimer Feld 229, D-69120 Heidelberg, Germany, and Organisch-Chemisches Institut, Universität Heidelberg, Im Neuenheimer Feld 270, D-69120 Heidelberg, Germany

Received June 18, 2009

Abstract: For a range of additions to alkynes gold is known to exhibit a much higher catalytic activity than a corresponding platinum compound. In order to approach the origin of this behavior we first investigate the propyne activation by the gold and platinum catalysts $AuCl_3$ and $PtCl_2(H_2O)$ where both metals possess a d^8 electron configuration and where the catalysts exhibit similar steric effects. Propyne serves as a representative for alkynes. Fully relativistic *ab initio* calculations of these alkyne-catalyst complexes are presented at the Dirac-Hartree−Fock self-consistent field (DHF-SCF), density functional theory (DFT/B3LYP), and Green's function (GF) level in order to properly account for the large relativistic effects of gold and platinum. For the alkyne/catalyst complexes both the perpendicular and in-plane conformations were studied as these possess very similar ground state energies and may easily transform into each other. Strongly varying orbital populations together with sizable energetic and structural differences of the frontier orbitals are found and can be considered as a major source of the differing catalytic activity. These mainly comprise vanishing LUMO densities at the carbon centers in the platinum complex together with increased LUMO energies making a nucleophilic attack harder than in the gold compound. As Green's function calculations show, DFT/B3LYP seems to overestimate correlation contributions leading to an unphysical energetic lowering of many unoccupied orbitals.

Introduction

Unactivated alkynes are not very reactive toward weak nucleophiles. This behavior changes significantly as soon as the C−C triple bond is activated by complexation with a suitable metal catalyst. In this context Hutchings first realized the ability of gold catalysts for the electrophilic alkyne activation[1] making the reaction with weak nucleophiles such as water, alcohols, or amines (Scheme 1) possible. In the meanwhile homogeneous gold catalysis grew into a major field of experimental as well as theoretical research[2−11] opening new pathways for a rich spectrum of organic compounds.

Scheme 1. Nucleophilic Addition on an Alkyne Activated by a Metal Catalyst

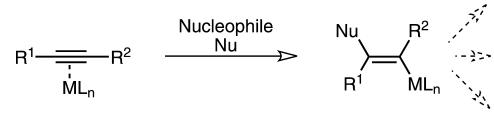

A striking experimental observation now is the considerable activity difference of gold and platinum catalysts as for example described for the gold-catalyzed phenol synthesis in refs 12 and 13. For this reaction calculations at the DFT level have been conducted,[14] and other computational investigations show similar results.[15]

In this work we first focus on the trisubstituted metal catalysts $AuCl_3$ and $PtCl_2(H_2O)$ because of their similarity with respect to *d*-orbital occupation, charge, and steric requirements. They both form a neutral complex with

* Corresponding author e-mail: Markus.Pernpointner@pci.uni-heidelberg.de.

† Theoretische Chemie, Universität Heidelberg.

‡ Organisch-Chemisches Institut.

10.1021/ct900441f CCC: $40.75
Published on Web 09/21/2009

Scheme 2. Structures (I) and (II) Show the π-like Perpendicular Orientation of the Propyne/Catalyst Complex whereas in the in-Plane Conformations (III) and (IV) a σ-type Bond between the Terminal Carbon Atom and the Metal Is Prevailing

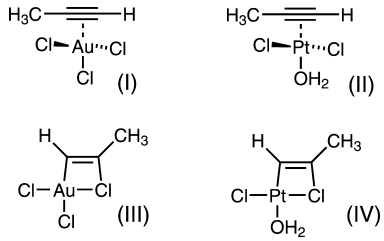

propyne and may be assumed to exhibit very similar properties. As we will show by fully relativistic *ab initio* methods this is, however, not the case. Due to the very small energetic differences both the perpendicular and in-plane orientation of the $AuCl_3/PtCl_2(H_2O)$ and propyne moieties depicted in Scheme 2 had to be considered. At a later stage the positively charged L-Au(I)/propyne complexes will be theoretically investigated taking into account their strongly varying properties of a positive charge and reduced steric requirements.

Both metals exhibit large relativistic effects (see e.g. ref 16 for a comprehensive review over the whole field) which are not only scalar in nature but also comprise considerable spin−orbit coupling. Additionally, electron correlation also contributes to the overall electron density distribution and cannot be treated separately from relativistic effects in heavy systems. For a consistent inclusion of all effects we therefore set out from the Dirac-Coulomb Hamiltonian and calculate the electronic and orbital structure at the Hartree−Fock self-consistent field (HF), density functional (DFT), and one-particle propagator (Green's function) methods. The calculations of the four structures in Scheme 2 were done at their numerically optimized equilibrium geometries.

Geometries and Computational Details

Since a geometry optimization at a four-component correlated level was beyond our computational capabilities, we generated equilibrium geometries for the structures in Scheme 2 at the one-component level. Hereby second-order Møller−Plesset (MP2) theory in combination with relativistic effective core potentials (RECP)[17] from the Stuttgart group was used in order to account for electron correlation and relativistic effects. It should be noted that the effect of spin−orbit coupling on the optimization of equilibrium geometries is neglected at this level of description but due to the closed-shell character of the complexes SO effects on equilibrium structures are assumed to be small. The basis sets were of cc-pVTZ quality for all atoms. It turned out that two energetically similar minimum geometries of the gold and platinum-alkyne complexes exist, namely the perpendicular and the in-plane conformation (see Scheme 2).

Table 1 shows the total energies (in atomic units) for the structures I-IV obtained at the MP2/RECP level of theory. Additionally, the energetic differences (in eV) between the perpendicular and in-plane conformations are given. It turns out that the energies of the two gold conformers are so similar that both structures may play a role in a reaction path of a nucleophilic attack, or in other words, that there is enough structural flexibility of the gold complex to switch from one orientation to the other during the nucleophilic attack. The two conformers of the platinum complex are energetically more separated with the consequence that a higher activation barrier has to be overcome if one conformation would be more suitable for a nucleophilic attack than the other. For the theoretical analysis of the nucleophilic attack we therefore investigate both geometries with respect to energetic and structural properties. All geometry optimizations for the perpendicular and in-plane conformations converged to C_s symmetry.

Table 1. Total MP2/RECP Energies (in au) of the Complexes I-IV[a]

$AuCl_3(Pr)_\perp$	$AuCl_3(Pr)_=$	Δ(eV)	$PtCl_2(H_2O)(Pr)_\perp$	$PtCl_2(H_2O)(Pr)_=$	Δ(eV)
−1630.864	−1630.866	0.06	−1231.354	−1231.332	−0.6

[a] The subscripts $\perp$ (=) correspond to the perpendicular (in-plane) conformation in Scheme 2. A positive sign hereby indicates a stability of the planar configuration versus the perpendicular one. (Pr) = propyne.

Table 2. Most Relevant Geometric Parameters for the Complexes I−IV Obtained at the MP2/RECP Level[a]

	$d(MC_1)$	$d(MC_2)$	$d(C_1C_2)$	$<(C_1C_2C_3)$	$<(HC_1C_2)$
Structure I(π)	2.162	2.197	1.242	170.6	166.8
Structure II(π)	2.024	2.040	1.268	161.5	158.0

	$d(MC_1)$	$d(MCl_1)$	$d(C_1C_2)$	$d(C_2Cl)$	$<(C_1C_2C_3)$	$<(HC_1C_2)$
Structure III(σ)	1.972	2.402	1.325	1.825	137.5	126.5
Structure IV(σ)	1.910	2.330	1.329	1.829	140.1	123.7

[a] All bond distances are in Å, all angles in degrees. The symbol (π) stands for the perpendicular orientations where the alkyne π orbitals are engaged in the bond to the metal and (σ) symbolizes the in-plane configuration.

In Table 2 we summarize the most important structural parameters of the alkyne/catalyst complexes obtained by the RECP/MP2 geometry optimization. This comprises the metal−carbon bond distances, the alkynylic carbon−carbon distance, and the bending of the carbon backbone.

For further analysis relativistic all-electron calculations at these optimized geometries were performed by using the DIRAC08 program package.[18] Suitable heavy-element basis sets which are adapted to the relativistic change in the electronic structure have to be applied and became available mainly by the work of Dyall.[19−26] From this repository a (22*s*19*p*12*d*10*f*1*g*) primitive set for gold and platinum was chosen. The basis sets both include one diffuse *f* and one core-correlating *g* function. Due to the large system size the recently developed infinite-order two-component (IOTC)[27] method was employed yielding nearly identical properties for the valence orbitals as a genuine four-component treatment. The two-electron spin−orbit contributions were hereby taken into account by the atomic mean-field approximation[28,29] also available in DIRAC08. As a consequence the orbitals

Table 3. HF and DFT Orbital Populations in Percent of the Perpendicular (⊥) Orientation of the Catalyst/Propyne Moiety Determined for the IOTC and Douglas-Kroll (DKINF) Hamiltonians[a]

method	orbital	$AuCl_3$...$Pr_\perp$	$PtCl_2(H_2O)$...$Pr_\perp$
IOTC	HOMO	94.5 Cl *p*, 3.9 C *p*	27.4 M *d*, 44.6 Cl *p*, 22.6 C *p*, 1.2 H *s*
HF	HOMO-1	8.6 M *d*, 88.8 Cl *p*	20.1 M *d*, 43.8 Cl *p*, 28.8 C *p*, 1.7 H *s*
DKINF	HOMO	95.2 Cl *p*, 3.8 C *p*	22.2 M *d*, 36.3 Cl *p*, 35.8 C *p*, 1.9 H *s*
HF	HOMO-1	8.3 M *d*, 88.7 Cl *p*, 2.2 C *p*	26.1 M *d*, 54.7 Cl *p*, 15.5 C *p*, 1.0 H *s*
IOTC	HOMO	94.7 Cl *p*, 4 C *p*	42.3 M *d*, 47.5 Cl *p*, 7.3 C *p*
DFT	HOMO-1	14.5 M *d*, 82.4 Cl *p*	34.1 M *d*, 42.2 Cl *p*, 18.1 C *p*, 1.0 H *s*
DKINF	HOMO	95.1 Cl *p*, 2.4 C *p*	37.7 M *d*, 59.6 Cl *p*, 1.1 C *p*
DFT	HOMO-1	12.3 M *d*, 86.1 Cl *p*	39.4 M *d*, 33.2 Cl *p*, 23.8 C *p*

[a] Contributions below one percent are not listed; M stands for metal which is either Au or Pt with the corresponding Mulliken charges of 0.815 and 0.731, respectively.

(spinors) become relaxed with respect to spin−orbit coupling also in the absence of the small-component basis which greatly reduces the numerical effort of the calculation.

In order to distinguish spin−orbit coupling effects from scalar relativistic effects the infinite-order Douglas-Kroll Hamiltonian (DKINF) was employed including relativity only at the scalar level. This is of great importance for the validation of one-component methods which consider only scalar relativistic effects by applying a RECP. Extensive potential energy surface and reaction path calculations can normally not be done at the four-component or even at the IOTC level.

The HOMO and LUMO orbitals obtained by IOTC and DKINF Hamiltonians were then visualized at the HF and DFT level (see Fossgaard et al. for a four-component realization of DFT[30]) in order to elucidate differences in the electronic structure of the gold and platinum complexes. For all relativistic calculations the B3LYP functional[31] was employed. Since DFT often uses parametrized functionals which may lead to constant shifts of the occupied Kohn−Sham orbital energies (see below) the fully relativistic propagator method[32,33] was applied yielding parameter-free correlation corrections to the occupied orbitals in the outer valence space. Propagator-based methods give access to final state distributions resulting from electron detachment/attachment or excitation processes (see for example refs 34−38 for an overview). This can be applied to determine the energies of the occupied valence orbitals including electron correlation and relativistic effects by calculating the corresponding ionization spectra of the complexes. As long as the one-particle picture remains valid (which is in general the case for valence ionizations) the final state energies reflect the positions of the occupied orbitals very accurately. If no electron correlation were taken into account the description would yield the Koopmans energies, but the propagator introduces the sought correlation corrections. It should be mentioned that corrections to the Koopmans energies can be obtained for occupied orbitals only. In this respect the propagator method is very useful to compare *ab initio* correlation shifts to DFT shifts (see discussion below). The numerical algorithm necessary for the solution of the propagator is based on the algebraic diagrammatic construction (ADC).[39]

Results and Discussion

The C≡C triple bond in the complexes is elongated from 1.214 Å in free propyne (optimized geometry at the MP2 level) to 1.242 Å (I), 1.268 Å (II), 1.325 (III), and 1.329 in (IV) clearly indicating an activation of the triple bond in the π-type complexes (I, II) and a substantial change to C−C double-bond (sp^2) character in the σ homologues (III, IV). The transition from a *sp* to a sp^2 hybridization on carbon is also reflected by a pronounced reduction of the $C_1C_2C_3$ bond angle from 170.6/161.5 degrees (π) to 137.5/140.1 degrees (σ). The HC_1C_2 angles in the σ complexes are even smaller and reflect the sp^2 character of the connected carbon atom. Despite the significant differences in the carbon hybridization and bonding type to the metal atom (σ/π) the total energies are unexpectedly similar as can be seen from the values given in Table 1.

The relativistic stabilization of the 6*s* shell together with a relativistic destabilization of the 5*d* shell in gold and platinum leads to a decreased 5*d*/6*s* gap enabling larger participation of the 5*d* orbitals in the chemical bonding. In gold, for example this energy gap amounts to 1.150 eV compared to the nonrelativistic value of 5.301 eV.[40] We therefore first investigate the metal 5*d* orbital contributions to the HOMO and HOMO-1 by a population analysis[41] in both complexes. It is known that the absolute values obtained by a Mulliken analysis exhibit some basis set dependency (see for example refs 42 and 43 for a good discussion of this problem), but the procedure is appropriate for comparative purposes as long as basis sets of the same quality and structure are employed for all species under investigation. Afterwards, the effect of electron correlation and spin−orbit splitting on orbital energies and densities will be analyzed.

Metal Populations in the Occupied Frontier Orbitals

We first concentrate on the perpendicularly oriented π-type complexes (I) and (II) of Scheme 2. From Table 3 it can be seen that despite their neighborhood in the periodic table the gold and platinum *d* orbital participations in the HOMOs of the complexes are substantially different at the HF and DFT level for both the IOTC and DKINF Hamiltonians.

In the transition metals Sc - Zn the 3*d* orbitals are more compact than in the corresponding 4*d* and 5*d* series and show much less participation in the outer valence space than the higher homologues.[44] Despite this, there is no Au 5*d* contribution to the HOMO even at the DFT level including electron correlation and only dominating chlorine *p* and weak carbon *p* character is found for the HOMO. The gold 5*d*

Table 4. HF and DFT Orbital Populations in Percent of the in-Plane (=) Orientation of the Catalyst/Propyne Moiety Determined for the IOTC and Douglas-Kroll (DKINF) Hamiltonians[a]

method	orbital	$AuCl_3$...$Pr_=$	$PtCl_2(H_2O)$...$Pr_=$
IOTC	HOMO	7.6 M *d*, 65.3 Cl *p*, 21.9 C *p*	25.3 M *d*, 8.3 Cl *p*, 53.2 C *p*, 3.6 H *s*
HF	HOMO-1	2.5 M *d*, 91.8 Cl *p*, 2.3 C *p*	6 M *s*, 50.2 M *d*, 38.5 Cl *p*, 1.3 C *p*
DKINF	HOMO	7.6 M *d*, 66.3 Cl *p*, 22.2 C *p*	21.2 M *d*, 8.1 Cl *p*, 59.1 C *p*, 3.9 H *s*
HF	HOMO-1	2.9 M *d*, 95 Cl *p*	39.9 M *d*, 58.5 Cl *p*
IOTC	HOMO	11.1 M *d*, 77.8 Cl *p*, 6.7 C *p*	59.7 M *d*, 20.5 Cl *p*, 11.4 C *p*
DFT	HOMO-1	5.7 M *d*, 89.1 Cl *p*, 1.6 C *p*	7.3 M *s*, 56.9 M *d*, 9.8 Cl *p*, 18.5 C *p*, 1.6 H *s*
DKINF	HOMO	9.7 M *d*, 80.2 Cl *p*, 7.9 C *p*	50.9 M *d*, 29.8 Cl *p*, 15.2 C *p*
DFT	HOMO-1	6.4 M *d*, 91.6 Cl *p*	48.9 M *d*, 6.7 Cl *p*, 28.7 C *p*, 1.9 H *s*

[a] Contributions below one percent are not listed; M stands for metal which is either Au or Pt with the corresponding Mulliken charges of 0.836 and 0.622, respectively.

contributions just appear moderately in the HOMO-1. This is in stark contrast to the situation of the platinum complex where the metal and carbon contributions together make up approximately 50% of the HOMO and HOMO-1 populations. This pronounced structural difference in the outer valence orbitals will also lead to modified LUMO densities giving rise to different affinities to the nucleophile (see next section for the density plots and the discussion of the energetic factors).

The next issue to be addressed is the influence of spin−orbit coupling on the populations. As mentioned before the IOTC Hamiltonian includes spin−orbit coupling for the valence orbitals to the same accuracy as a fully four-component treatment,[27] whereas the infinite order Douglas-Kroll ansatz (DKINF) only treats scalar relativistic effects. One can therefore extract information about the influence of SO-coupling by comparing results obtained by these two Hamiltonians. In the gold complex hardly any effect of SO-coupling is observed at the HF level of theory, and inclusion of electron correlation via DFT does not introduce much of an alteration. This result points to a low sensitivity of the Au-propyne complex toward SO-coupling justifying a scalar relativistic treatment. In the platinum complex, however, we observe significantly larger population changes when going from the IOTC to the DKINF Hamiltonian at both levels of electronic structure treatment (HF, DFT). As a consequence, a purely scalar relativistic description for the platinum complex is not accurate enough for the correct reproduction of the orbital populations but may still be useful if orbital energies and HOMO/LUMO densities change only negligibly upon inclusion of SO coupling.

Due to the sensitivity of transition metal *d* electrons toward electron correlation one may expect substantial changes in the corresponding *d* populations as soon as a DFT treatment is applied for the electronic structure. This is indeed the case for the platinum-propyne HOMO and HOMO-1 using the IOTC and DKINF description of relativity. For both Hamiltonians a substantial increase of the Pt 5*d* population is observed during the transition from a HF to a DFT treatment (for example, the largest change of 15.5% occurs for the HOMO obtained by the DKINF Hamiltonian). For the gold compound, however, neither the HOMOs acquire *d* character (in fact, the overall populations hardly change at all) nor is the *d* increase in the HOMO-1 as pronounced as in the platinum case (a maximum change of 5.9% occurs in the HOMO-1/IOTC case). A significantly lower participation of the Au 5*d* orbitals in the valence space and a reduced sensitivity of these orbitals toward electron correlation may reflect a more compact *d* orbital structure in the gold complex. Another observation is the substantial depletion of carbon character in the platinum complex HOMOs in favor of metal *d* contributions upon inclusion of electron correlation via DFT.

For the perpendicularly oriented complexes (I) and (II) we summarize our findings as follows: The populations of the gold complex show only a weak sensitivity to spin−orbit coupling and electron correlation, and the *d* orbitals play a less important role for the highest and second highest occupied molecular orbital in all treatments. In contrast, the carbon and platinum *d* populations change significantly upon inclusion of electron correlation and SO coupling leading to altered LUMO structures as well. The pronounced platinum 5*d* participation in the outer valence orbitals was also observed in a number of previously calculated dianionic complexes of the $PtX_{4,6}^{2-}$ type (X=F, Cl) where one would normally expect a prevailing ligand population.[45]

We next analyze the orbital populations of the in-plane structures (III) and (IV) of Scheme 2 that can be found in Table 4.

At first we now observe a gold 5*d* HOMO contribution between 7.6% and 11.1% for all Hamiltonians and methods which is in contrast to the results for the perpendicularly oriented Au/Pr complex. Despite the altered overall populations the same insensitivity to SO coupling is visible in the gold complex comparing the results for the IOTC and DKINF Hamiltonian. However, switching from HF to DFT leads to a remarkable reduction of the HOMO carbon contribution and only to a minor increase of the gold 5*d* population. As it was the case for the perpendicular complexes the platinum species also exhibits a higher sensitivity to SO coupling and a very pronounced change of the 5*d* character including electron correlation both in the HOMO and HOMO-1. From the results above we observe substantial differences between the gold and platinum complexes both in the perpendicular as well as the in-plane configuration which will have an impact on the affinity toward a nucleophile. Structural factors are mainly based on the different composition of the outer valence orbitals.

The $AuCl_3$ and $PtCl_2(H_2O)$ fragments of the compounds (I) and (II) have also been calculated separately in order to reveal similar trends in the isolated species as occurring in the complexes. Considering the metal *d* populations we observe the same pronounced Pt *d* orbital participation to the three highest occupied orbitals, namely 26.7% (HOMO),

Table 5. Orbital Energies at Various Levels of Theory in eV of (a) the Perpendicular Au/Pr Complex and (b) the Perpendicular Pt/Pr Complex

orbital	IOTC/HF	DKINF/HF	IOTC/DFT	DKINF/DFT	IOTC/ADC(3)
		(a) $AuCl_3$...$Pr_\perp$			
LUMO+3	1.442	1.452	−0.583	0.582	-
LUMO+2	1.045	1.046	−1.119	−1.120	-
LUMO+1	0.765	0.766	−2.014	−2.001	-
LUMO	−0.220	−0.288	−3.820	−3.845	-
HOMO	−11.072	−11.075	−7.627	−7.630	−10.218
HOMO−1	−11.456	−11.524	−7.796	−7.850	−10.646
GAP	10.852	10.786	3.807	3.785	-
		(b) $PtCl_2(H_2O)$...$Pr_\perp$			
LUMO+3	2.151	2.152	−0.105	−0.112	-
LUMO+2	1.682	1.690	−0.630	−0.629	-
LUMO+1	1.445	1.445	−1.008	−1.014	-
LUMO	1.173	1.174	−1.800	−1.807	-
HOMO	−9.844	−9.959	−6.275	−6.427	−8.676
HOMO−1	−10.119	−10.074	−6.638	−6.506	−9.060
GAP	11.018	11.133	4.475	4.620	-

14.3% (HOMO-1), and 18.9% (HOMO-2). In $AuCl_3$ the corresponding *d* character is significantly lower and amounts to 4.4% (HOMO), 7.7% (HOMO-1), and 5.2% (HOMO-2), a behavior which is resembled in the complexes. If one compares the Mulliken charges of the metal centers in the free catalyst and in the complex a small depletion of electron density is observable (0.81 → 0.95 for the Au center and 0.73 → 0.82 for the Pt center). The focus in this work, however, predominantly lies on the analysis of the corresponding alkyne/catalyst complexes and their reactivity toward a nucleophile. For an in-depth analysis of the isolated species we therefore refer to e.g. ref 46.

Energetics and HOMO/LUMO Structures

Considering the orbital energies and structures we first focus on the perpendicular complexes. Table 5a,b contains the corresponding orbital energies for all Hamiltonians and methods. At first we look at the influence of SO coupling on the orbital energies by forming a total average deviation $\Delta\varepsilon_{av}$ spanning the range HOMO-1... LUMO+3. $\Delta\varepsilon_{av}$ is calculated as the sum of all differences $|\varepsilon^{HF}_{IOTC} - \varepsilon^{HF}_{DKINF}|$ and $|\varepsilon^{DFT}_{IOTC} - \varepsilon^{DFT}_{DKINF}|$ divided by the number of orbitals taken into account. For the gold complex we obtain a quite low average deviation of $\Delta\varepsilon_{av} = 0.021$ eV which is not too surprising due to the small population changes upon SO coupling. Despite the considerably larger alterations in the orbital populations $\Delta\varepsilon_{av}$ for the platinum complex increases only up to 0.04 eV where the largest contribution stems from the HOMOs. The direct influence of SO coupling on the highest occupied and lowest virtual orbitals is therefore small.

An important fact is the negative first LUMO energy in the Au/Pr complex at the IOTC/HF and DKINF/HF level reflecting a high affinity toward a nucleophile and the capability to stabilize an excess electron whereas the Pt/Pr complex does not possess a negative LUMO energy. This situation changes pronouncedly when electron correlation is taken into account via DFT. At first the HOMO/LUMO gap is substantially reduced from 10.9 to 3.8 eV in the gold complex and from 11.0 to 4.5 eV in the platinum complex stressing large electron correlation effects. An even more striking fact, however, is now the decrease of all LUMO energies below zero which would indicate a substantially increased affinity of both complexes toward nucleophiles and a possibility to bind even more than one excess electron. According to the lower-lying LUMOs of the Au/Pr complex this species still forms an even stronger bond to the nuclophile than the platinum complex, but four negative LUMO energies for a neutral closed shell system do not seem to be very reliable. This behavior most probably has its origin in the difficult interpretation of DFT Kohn−Sham (KS) orbital energies.

The Kohn−Sham (KS) formulation of DFT[47] produces one-particle functions (orbitals or spinors in the relativistic DFT) that incorporate electron exchange and correlation effects through the corresponding functionals. However, the interpretation of these orbitals is not undisputed. On the one hand they are seen as purely mathematical constructs in order to reproduce the total electronic density ρ[48] where on the other hand a physical meaning is attributed to them due to the corresponding physical nature of the Kohn−Sham potential.[49,50] If one looks at the occupied orbitals, only the KS-HOMO energy has the physical meaning of the (negative) lowest vertical ionization potential,[51−57] whereas the other are seen as merely auxiliary quantities.[48] Building on the empirical observation that approximate Kohn−Sham energies for the occupied orbitals exhibit a substantial but nearly constant shift with respect to the experimental ionization energies,[58,59] Chong, Gritsenko, and Baerends developed the concept of relaxed vertical ionization potentials (VIPs) and showed a very good agreement of those to the KS orbital energies.[60] In addition, Gritsenko, Braïda, and Baerends[61] analyzed the connection between KS and Dyson orbital theories in the ionization process being relevant for a detailed understanding of the $\varepsilon - I$ relations. In order to estimate this constant shift of the KS orbital energies in our systems we performed fully relativistic propagator calculations of the HOMO energies at the IOTC/ADC(3) level and observe a substantial overestimation of correlation contributions in the DFT treatment (2.6 eV for the Au/Pt and 2.4 eV for the Pt/Pr complex compared to the IOTC/DFT values). As a consequence, the LUMO energies also incorporate this correlation error making the strongly negative orbital energies at the IOTC and DKINF level less troublesome. It should also be mentioned that the approximate functionals may suffer from shortcomings due to self-interaction errors in particular associated with the electron-rich *d* shells. Considering the related DFT-LUMO densities one therefore has to interpret them with care.

For further analysis it is more comprehensive to look at pictorial representations of the HOMO−LUMO orbital densities instead of tabulating dominant basis function coefficients. We commence by displaying the HOMO densities of the perpendicular gold (left) and platinum (right) complexes (I) and (II) at the IOTC/HF level in Figure 1.

In both complexes the occupied alkynylic π orbital and the chlorine lone pairs are clearly visible. The HOMOs obtained at the IOTC/DFT, DKINF/HF, and DKINF/DFT level of theory look nearly identical to the IOTC/HF HOMO

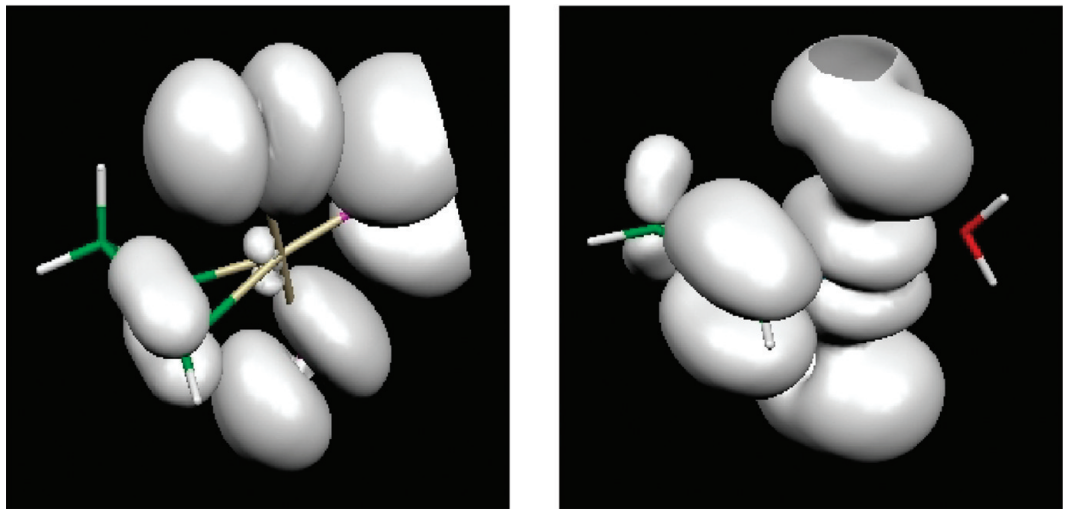

Figure 1. HOMO orbital densities for the perpendicular Au/Pr (left) and Pt/Pr (right) complex at the IOTC/HF level. The methyl group is directed away from the observer.

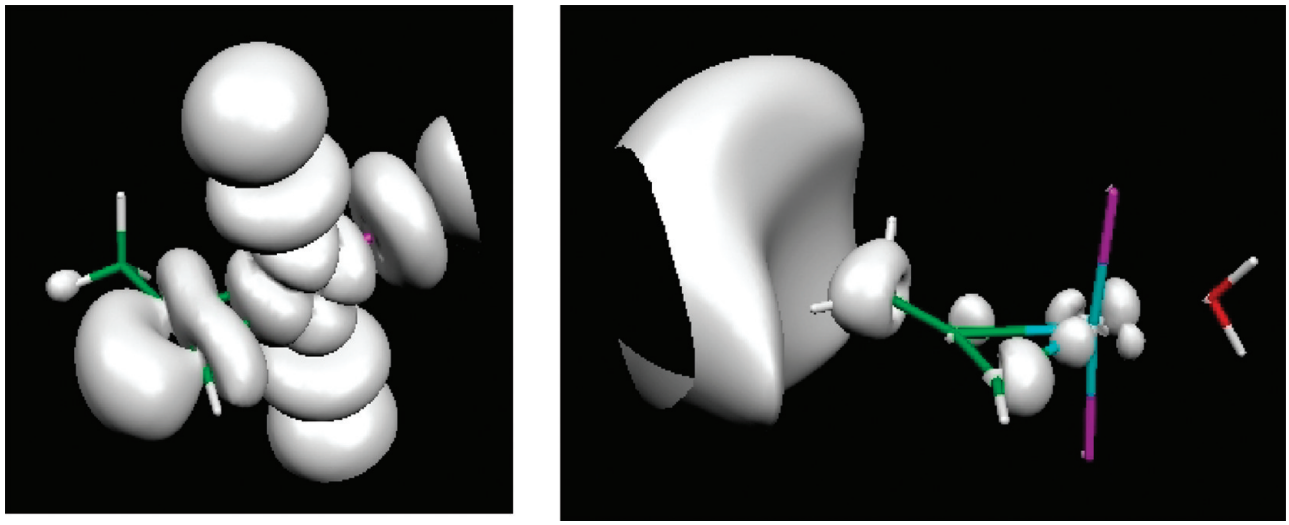

Figure 2. LUMO orbital densities of the Au/Pr (left) and Pt/Pr (right) complex at the IOTC/HF level. The different orbital densities at the alkynylic carbon atoms are clearly visible.

for both complexes and need not be displayed separately. One of the most prominent differences between the perpendicularly oriented Au and Pt complexes is the differing LUMO density obtained at the IOTC/HF level (see Figure 2) which provides a reasoning for the ease of a nucleophilic attack on the Au/Pr carbyne centers. In contrast, a nonexistent Pt/Pr LUMO density at these carbon centers will not lead to a good overlap of the nucleophile frontier orbital and the complex. As a consequence, a nucleophilic attack on one of the Pt/Pr carbyne centers is less promoted. Looking at the Mulliken charges of the propyne carbon atoms (see Table 7) reveals that the C_2 atom always bears the highest positive charge favoring a Markovnikov addition regardless of available LUMO densities.

This different behavior toward the nucleophile is in line with the negative (positive) LUMO energy of the gold (platinum) complex. The effect of electron correlation (treated at the DFT level of theory) will certainly influence the LUMO densities which are visualized in Figure 3. There the IOTC/DFT LUMO densities at the carbyne atoms of both complexes now show a close resemblance and do not provide a clear-cut argument for the observed affinity difference. From the considerations above one should keep in mind, however, that the DFT HOMO/LUMO energies bear intrinsic shifts, and the corresponding

Table 6. Orbital Energies at Various Levels of Theory in eV of the (a) in-Plane Au/Pr Complex and (b) the in-Plane Pt/Pr Complex

orbital	IOTC/HF	DKINF/HF	IOTC/DFT	DKINF/DFT	IOTC/ADC(3)
		(a) $AuCl_3$...$Pr_=$			
LUMO+3	1.445	1.442	−0.604	−0.607	-
LUMO+2	1.443	1.438	−1.305	−1.308	-
LUMO+1	0.884	0.880	−1.457	−1.453	-
LUMO	0.107	0.055	−3.613	−3.640	-
HOMO	−10.720	−10.743	−7.236	−7.277	−9.608
HOMO−1	−10.957	−10.920	−7.417	−7.361	−9.907
GAP	10.827	10.798	3.623	3.637	-
		(b) $PtCl_2(H_2O)$...$Pr_=$			
LUMO+3	1.990	1.988	−0.304	−0.308	-
LUMO+2	1.947	1.954	−0.383	−0.406	-
LUMO+1	1.863	1.860	−0.543	−0.509	-
LUMO	1.264	1.262	−1.107	−1.119	-
HOMO	−9.252	−9.336	−5.980	−6.182	−8.072
HOMO−1	−9.705	−9.932	−6.077	−6.242	−8.244
GAP	10.516	10.598	4.872	5.063	-

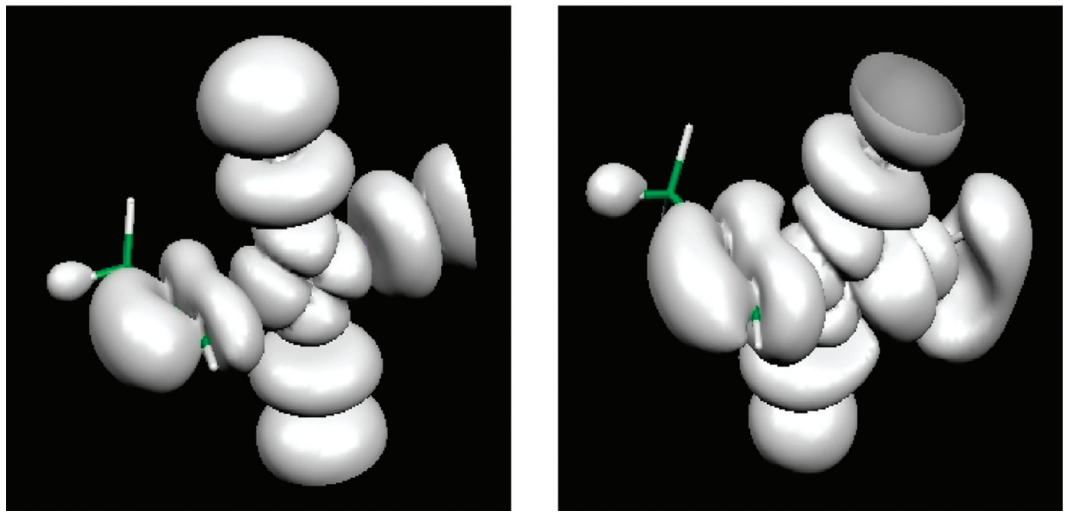

Figure 3. LUMO orbital densities of the Au/Pr (left) and Pt/Pr (right) complex at the IOTC/DFT level. The LUMO density differences are now blurred.

Table 7. Mulliken Charges at the DFT/B3LYP and HF Level Using Relativistic ECPs[a]

method	C_1	C_2	C_3
$Au_{\perp}$ B3LYP	+0.001	+0.0522	−0.273
HF	−0.049	+0.0529	−0.274
$Au_{=}$ B3LYP	−0.122	+0.0317	−0.263
HF	−0.155	+0.0319	−0.244
$Pt_{\perp}$ B3LYP	−0.175	+0.0489	−0.274
HF	−0.221	+0.0393	−0.259
$Pt_{=}$ B3LYP	−0.226	+0.0201	−0.275
HF	−0.315	+0.0387	−0.253
C_3H_4 HF	−0.199	−0.0747	−0.2752

[a] Au (Pt) stands for the gold (platinum)/propyne complex and ⊥ (=) for the perpendicular (in-plane) orientation. The charges of free propyne are given in the last line. The metal-induced activation of the C_2 atom toward a nucleophilic attack is clearly visible.

densities may therefore also deviate considerably from the actual situation. For this reason we do not establish our reasoning purely on DFT results.

In the last paragraph of this section we discuss the in-plane complexes whose orbital energies are shown in Table 6a,b at various levels of theory.

Despite the different hybridization of the propyne carbon atoms similar global trends as in the perpendicular configurations can be observed. The HOMO and LUMO energies are again all lower in the Au/Pr complex than in the corresponding Pt/Pr compound, and inclusion of electron correlation leads to a similarly large increase of the HOMO and decrease of the LUMO energies. For the determination of the shift introduced by DFT we again compare the IOTC/DFT HOMO energy in both complexes to the IOTC/ADC(3) value and obtain 2.4 eV for the Au/Pr and 2.1 eV for the Pt/Pr complex. In contrast to the perpendicular gold complex no negative first LUMO energy is obtained at the IOTC/HF and DKINF/HF level. Naturally the question arises if any affinity differences can be associated with the configurational change from perpendicular to in-plane or if it is related to the type of catalyst. To answer this we again visualize the corresponding orbital densities for the in-plane configurations.

In Figure 4 showing the IOTC/HF HOMO densities of the in-plane Au/Pr and Pt/Pr complexes we do not observe a substantial difference at the alkynylic carbon atoms and very similar plots (not displayed) also result in a scalar relativistic DKINF/HF treatment. From Figure 5 we see the same depletion of LUMO density at the carbyne atoms of the in-plane platinum complex calculated at the IOTC/HF level. This difference is therefore related to the catalyst (gold or platinum center) and not to the orientation of the alkyne moiety. According to the nonexistent HF LUMO density on the carbyne positions the Pt/Pr complex should exhibit a decreased affinity to the nucleophile. The increased affinity of the gold complex is also reflected by a considerably lower LUMO energy of +0.107 eV compared to +1.264 eV in the platinum complex.

The visualizations of the KS HOMOs using the IOTC and DKINF Hamiltonians will not introduce new information and are omitted. In all cases the KS orbital densities at the carbyne centers look very similar to the HF results, and SO coupling does not alter this picture. This is not the case with the LUMO densities depicted in Figure 6 at the IOTC/DFT level going in line with the findings for the perpendicular configurations. As before, the difference in the LUMO densities at the carbon atoms of both complexes is wiped out and does not allow for a clear structural argument with respect to affinities.

From this structural analysis we deduce that the type of catalyst (Au or Pt) influences the electronic structure and the densities at the reactive centers much more than the geometric orientation of the two building blocks even if the latter implies a change of the carbon hybridization. However, due to its negative LUMO energy the perpendicular gold complex clearly alleviates a nucleophilic attack, whereas a reorientation in the platinum compound does not exhibit a comparable behavior. The low energy barrier of 0.06 eV for a transformation between the two orientations of Au/Pr leads to nucleophilic reactions where only the perpendicular type is involved. This may be of relevance for further mechanistic studies of the nucleophilic attack.

In total we can summarize our findings as follows. Spin−orbit coupling has a considerable influence on the orbital populations in the Pt-containing complexes but leaves the outer valence compositions in the corresponding gold species nearly unaltered. Orbital energies of both complexes are hardly modified upon

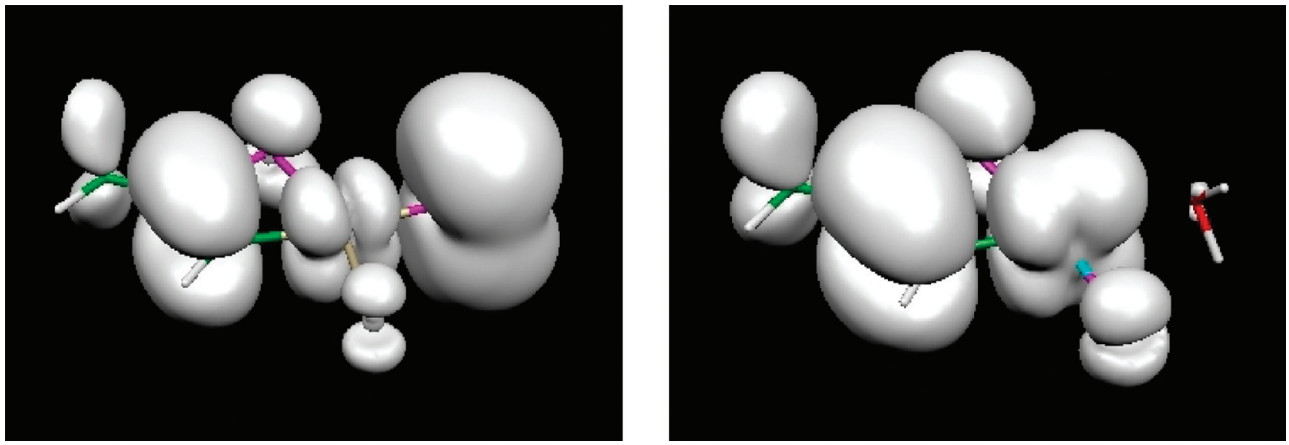

Figure 4. HOMO orbital densities for the in-plane Au/Pr (left) and Pt/Pr (right) complex at the IOTC/HF level. The methyl group is directed away from the observer.

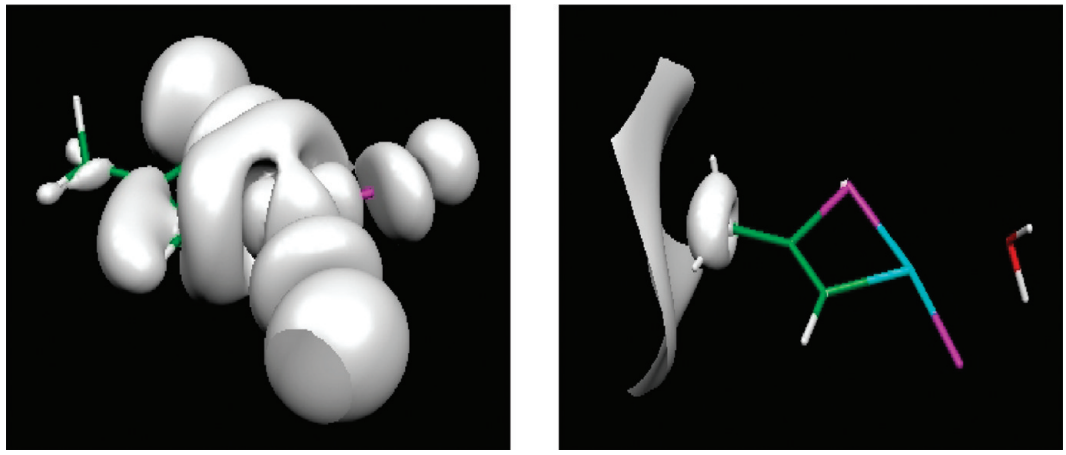

Figure 5. LUMO orbital densities for the in-plane Au/Pr (left) and Pt/Pr (right) complex at the IOTC/HF level.

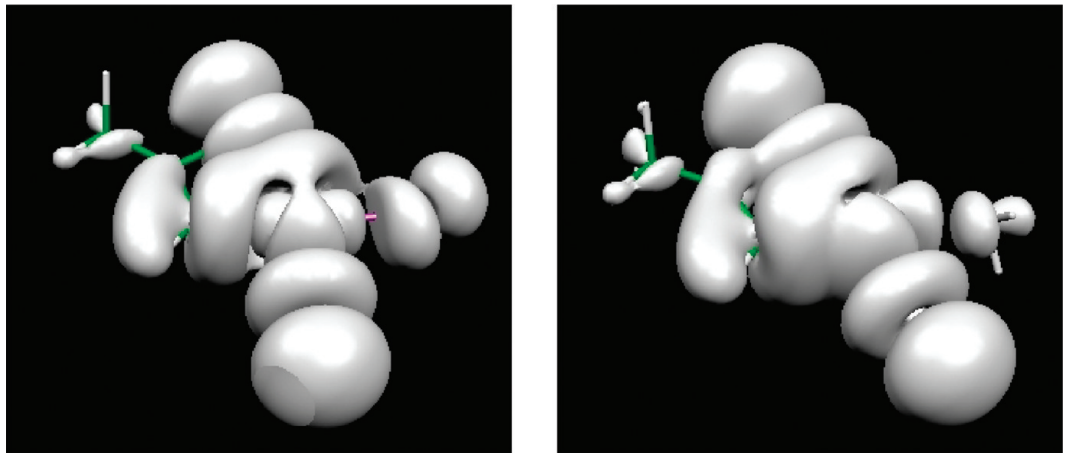

Figure 6. LUMO orbital densities for the in-plane Au/Pr (left) and Pt/Pr (right) complex at the IOTC/DFT level. The methyl group is directed away from the observer.

inclusion of SO coupling which is understandable due to their closed-shell character. Very differing metal *d* populations in the outer valence space lead to large structural alterations in the LUMOs which can be considered as one main ingredient for the different catalytic efficiency. Hereby no carbon LUMO density was found for the platinum complexes making an overlap with a nucleophilic frontier orbital unfavorable. In contrast to that both gold complexes exhibit a high LUMO density together with considerably lower LUMO energies alleviating a nucleophilic attack both from the structural as from the energetic point of view. The orientation of the propyne moiety (perpendicular or in-plane) is hereby irrelevant. Electron correlation treated at the relativistic DFT level has a major impact on orbital energies, populations, and densities. The interpretation of the DFT results especially with respect to virtual orbital energies is not straightforward as discussed in the text, and relativistic propagator calculations reveal a considerable overestimation of correlation effects by DFT. Therefore the obtained DFT-LUMO densities cannot serve as an unambiguous basis for the structural analysis. For all four species under consideration the

central carbon atom bears the highest positive charge, and a Markovnikov-type attack is therefore most probable.

Acknowledgment. The authors would like to thank Dr. R. Bast for technical assistance with the visualization module of DIRAC.

References

(1) Hutchings, G. J. *J. Catal.* **1985**, *96*, 292.

(2) Dyker, G. *Angew. Chem.* **2000**, *112*, 4407.

(3) Dyker, G. *Angew. Chem., Int. Ed. Engl.* **2000**, *39*, 4237.

(4) Hashmi, A. S. K. *Gold Bull.* **2003**, *36*, 3.

(5) Hashmi, A. S. K. *Gold Bull.* **2004**, *37*, 51.

(6) Hofmann-Röder, A.; Krause, N. *Org. Biomol. Chem.* **2005**, *3*, 387.

(7) Hashmi, A. S. K. *Angew. Chem.* **2005**, *117*, 7150.

(8) Hashmi, A. S. K. *Angew. Chem., Int. Ed. Engl.* **2005**, *44*, 6990.

(9) Hashmi, A. S. K.; Hutchings, G. *Angew. Chem.* **2006**, *118*, 8064.

(10) Hashmi, A. S. K.; Hutchings, G. *Angew. Chem., Int. Ed. Engl.* **2006**, *45*, 7896.

(11) Hashmi, A. S. K. *Chem. Rev.* **2007**, *107*, 3180.

(12) Hashmi, A. S. K.; Weyrauch, J. P.; Rudolph, M.; Kurpejovic, E. *Angew. Chem.* **2004**, *116*, 6707.

(13) Hashmi, A. S. K.; Weyrauch, J. P.; Rudolph, M.; Kurpejovic, E. *Angew. Chem., Int. Ed. Engl.* **2004**, *43*, 6545.

(14) Martin-Matute, B.; Nevado, C.; Cárdenas, D. J.; Echavarren, A. M. *J. Am. Chem. Soc.* **2003**, *125*, 5757.

(15) Soriano, E.; Marco-Contelles, J. *Organometallics* **2006**, *25*, 4542.

(16) *Relativistic Electronic Structure Theory*; Schwerdtfeger, P., Ed.; Elesevier B. V.: Amsterdam, 2004.

(17) Figgen, D.; Rauhut, G.; Dolg, M.; Stoll, H. *Chem. Phys.* **2005**, *311*, 227.

(18) Visscher, L.; Jensen, H. J. A.; Saue, T. *Dirac, a relativistic ab initio electronic structure program, Release DIRAC08 (2008)*,with new contributions from Bast, R., Dubillard, S., Dyall, K. G., Ekström, U., Eliav, E., Fleig, T., Gomes, A. S. P., Helgaker, T. U., Henriksson, J., Iliaš, M., Jacob, Ch. R., Knecht, S., Norman, P., Olsen, J., Pernpointner, M., Ruud, K., Sałek, P., Sikkema, J. (see http://dirac.chem.sdu.dk (accessed September 1, 2009)).

(19) Dyall, K. G. *Theor. Chem. Acc.* **1998**, *99*, 366.

(20) Dyall, K. G. *Theor. Chem. Acc.* **2002**, *108*, 335.

(21) Dyall, K. G. *Theor. Chem. Acc.* **2002**, *108*, 365.

(22) Dyall, K. G. *Theor. Chem. Acc.* **2003**, *109*, 284.

(23) Dyall, K. G. *Theor. Chem. Acc.* **2004**, *112*, 403.

(24) Dyall, K. G. *Theor. Chem. Acc.* **2006**, *115*, 441.

(25) Dyall, K. G. *Theor. Chem. Acc.* **2007**, *117*, 483.

(26) Dyall, K. G. *Theor. Chem. Acc.* **2007**, *117*, 491.

(27) Iliaš, M.; Saue, T. *J. Chem. Phys.* **2007**, *126*, 064102.

(28) Hess, B. A.; Marian, C. M.; Wahlgren, U.; Gropen, O. *Chem. Phys. Lett.* **1996**, *251*, 365.

(29) Iliaš, M.; Kellö, V.; Visscher, L.; Schimmelpfennig, B. *J. Chem. Phys.* **2001**, *115*, 9667.

(30) Fossgaard, O.; Gropen, O.; Corral Valero, M.; Saue, T. *J. Chem. Phys.* **2003**, *118*, 10418.

(31) Stephens, P. J.; Devlin, J. F.; Chabalowski, C. F.; Frisch, M. J. *J. Phys. Chem.* **1994**, *98*, 11623.

(32) Pernpointner, M.; Trofimov, A. B. *J. Chem. Phys.* **2004**, *120*, 4098.

(33) Pernpointner, M. *J. Chem. Phys.* **2004**, *121*, 8782.

(34) Abrikosov, A. A.; Gorkov, L. P.; Dzyaloshinski, I. E. *Methods of Quantum Field Theory in Statistical Physics*; Prentice-Hall: Englewood Cliffs, 1963.

(35) Fetter, A. L.; Walecka, J. D. *Quantum Theory of Many-Particle Systems*; McGraw-Hill: New York, 1971.

(36) Mattuck, R. D. *A Guide to Feynman Diagrams in the Many-Body Problem*; McGraw-Hill: New York, 1967.

(37) Cederbaum, L. S.; Domcke, W. *Adv. Chem. Phys.* **1977**, *36*, 205.

(38) Cederbaum, L. S.; Domcke, W.; Schirmer, J.; von Niessen, W. *Adv. Chem. Phys.* **1986**, *65*, 115.

(39) Schirmer, J.; Cederbaum, L. S.; Walter, O. *Phys. Rev. A* **1983**, *28*, 1237.

(40) Eliav, E.; Kaldor, U.; Ishikawa, Y. *Phys. Rev. A* **1994**, *49*, 1724.

(41) Mulliken, R. S. *J. Chem. Phys.* **1955**, *23*, 1833.

(42) Wiberg, K. B.; Rablen, P. R. *J. Comput. Chem.* **1993**, *14*, 1504.

(43) Meister, J.; Schwarz, W. H. E. *J. Phys. Chem.* **1994**, *98*, 8245.

(44) Frenking, G.; Fröhlich, N. *Chem. Rev.* **2000**, *100*, 717.

(45) Pernpointner, M.; Rapps, T.; Cederbaum, L. S. *J. Chem. Phys.* **2008**, *129*, 174302.

(46) Hargittai, M.; Schulz, A.; Réffy, B.; Kolonits, M. *J. Am. Chem. Soc.* **2001**, *123*, 1449.

(47) Kohn, W.; Sham, L. J. *Phys. Rev.* **1965**, *140*, A1133.

(48) Parr, R. G.; Yang, W. *Density Functional Theory of Atoms and Molecules*; New York: Oxford University Press, 1989.

(49) Baerends, E. J.; Gritsenko, O. V. *J. Phys. Chem. A* **1997**, *101*, 5383.

(50) Baerends, E. J. *Theor. Chem. Acc.* **2000**, *103*, 1265.

(51) Perdew, J. P.; Parr, R. G.; Levy, M.; Balduz, J. L. *Phys. Rev. Lett.* **1982**, *49*, 1691.

(52) Perdew, J. P.; Levy, M. *Phys. Rev. Lett.* **1983**, *51*, 1884.

(53) Levy, M.; Perdew, J. P.; Sahni, V. *Phys. Rev. A* **1984**, *30*, 2745.

(54) Almbladh, C. O.; Pedroza, A. C. *Phys. Rev. A* **1984**, *29*, 2322.

(55) Almbladh, C. O.; von Barth, U. *Phys. Rev. B* **1985**, *31*, 3231.

(56) Perdew, J. P.; Levy, M. *Phys. Rev. B* **1997**, *56*, 16021.

(57) Casida, M. *Phys. Rev. B* **1998**, *59*, 4694.

(58) Baerends, E. J.; Ros, P. *Chem. Phys.* **1973**, *2*, 52.

(59) Politzer, P.; Abu-Awwad, F. *Theor. Chem. Acc.* **1998**, *99*, 83.

(60) Chong, D. P.; Gritsenko, O. V.; Baerends, E. J. *J. Chem. Phys.* **2002**, *116*, 1760.

(61) Gritsenko, O. V.; Braïda, B.; Baerends, E. J. *J. Chem. Phys.* **2003**, *119*, 1937.

CT900441F